

Nonlocal Effects and Shrinkage of the Vortex Core Radius in $\text{YNi}_2\text{B}_2\text{C}$ Probed by μSR

K. Ohishi, K. Kakuta and J. Akimitsu

Department of Physics, Aoyama-Gakuin University, Setagaya-ku, Tokyo 157-8572, Japan

W. Higemoto and R. Kadono[†]

*Institute of Materials Structure Science, High Energy Accelerator Research Organization (KEK),
Tukuba, Ibaraki 305-0801, Japan*

J. E. Sonier

Department of Physics, Simon Fraser University, Burnaby, British Columbia, Canada V5A 1S6

A. N. Price, R. I. Miller, and R. F. Kiefl

TRIUMF and Department of Physics, University of British Columbia, Vancouver, British Columbia, Canada V6T 1Z1

M. Nohara, H. Suzuki and H. Takagi

*Graduate School of Frontier Sciences, University of Tokyo, Bunkyo-ku, Tokyo 113-8656, Japan
(November 1, 2018)*

The magnetic field distribution in the vortex state of $\text{YNi}_2\text{B}_2\text{C}$ has been probed by muon spin rotation (μSR). The analysis based on the London model with nonlocal corrections shows that the vortex lattice has changed from hexagonal to square with increasing magnetic field H . At low fields the vortex core radius, $\rho_v(H)$, decreases with increasing H much steeper than what is expected from the \sqrt{H} behavior of the Sommerfeld constant $\gamma(H)$, strongly suggesting that the anomaly in $\gamma(H)$ primarily arises from the quasiparticle excitations outside the vortex cores.

74.60.Ec, 74.60.-w, 76.75.+i

The recent studies of the flux-line lattice (FLL) state in ordinary s -wave superconductors have revealed that the electronic structure of vortices is much more complicated than that of a simple array of rigid cylinders containing normal electrons. One of the unexpected phenomena within this conventional model is the non-linearity in the magnetic field dependence of the Sommerfeld constant $\gamma(H)$ (electronic specific heat coefficient) observed in CeRu_2^1 , NbSe_2^2 , and $\text{YNi}_2\text{B}_2\text{C}^2$. According to the above simple model where the quasiparticle excitations are confined within the cores of vortices (with a radius ξ) in s -wave superconductors, one would expect that $\gamma(H)$ is proportional to the number of vortices per unit cell and thus to the applied magnetic field H . However, experiments have revealed that this is not the case for any of the above compounds.^{1,2} Instead, they find a field dependence like $\gamma(H) \propto \sqrt{H}$ which is expected for d -wave superconductors having more extended quasiparticle excitations along nodes in the energy gap. The recent study on the effect of doping in $\text{YNi}_2\text{B}_2\text{C}$ and NbSe_2 indicates that the anomalous field dependence is observed only in the clean limit², suggesting the importance of nonlocal effects in understanding the field dependence of $\gamma(H)$. Moreover, it has been reported that the vortex core radius depends on applied magnetic field and shrinks at higher fields in NbSe_2^3 and in CeRu_2^4 .

Another complication especially for borocarbides ($\text{RNi}_2\text{B}_2\text{C}$, R = rare earth) is that a square FLL is formed in some of these compounds at high magnetic fields, whereas a hexagonal FLL is realized at low fields.⁵⁻⁸ This is not expected for the local model with isotropic inter-

vortex interactions and thereby suggests the importance of considering electronic structure (or the Fermi surface) and the associated nonlocal corrections in the specific compound.

We report on μSR measurements of the magnetic field dependence of the \hat{a} - \hat{b} magnetic penetration depth λ , the effective vortex core radius ρ_v , and the apex angle of the FLL θ in single crystalline $\text{YNi}_2\text{B}_2\text{C}$. We demonstrate that the proper reconstruction of the field profile with a square FLL is obtained from the μSR spectra only when the nonlocal corrections are considered.⁹ The field dependence of λ turned out to be linear over the entire magnetic field range of observation. More importantly, it was found that ρ_v shrinks sharply with increasing magnetic field and levels off at higher fields. This shrinkage, however, is much steeper than that expected for the case when the \sqrt{H} behavior of $\gamma(H)$ is entirely attributed to that of ρ_v , strongly suggesting that the anomaly in $\gamma(H)$ is mostly from the quasiparticle excitations outside the vortex cores.

The single crystal of $\text{YNi}_2\text{B}_2\text{C}$ used in this experiment (residual resistivity ratio, or rrr $\simeq 37.4$) had a surface area of $\sim 64 \text{ mm}^2$. The superconducting transition temperature T_c and the upper critical field H_{c2} ($T = 3 \text{ K}$) determined from resistivity and specific heat measurements were 15.4 K and 7.0 T, respectively.² μSR experiments were performed on the M15 and M20 surface muon beamlines at TRIUMF. An experimental setup with high timing resolution was employed to measure the transverse field (TF-) μSR time spectra up to 5 T. The sample was mounted with its \hat{c} -axis parallel to the applied field and

beam directions, while the initial muon spin polarization was perpendicular to the applied field. The sample was field cooled at the measured magnetic fields to minimize disorder of the FLL due to flux pinning. Since the muons stop randomly on the length scale of the FLL, the muon spin precession signal provides a random sampling of the internal field distribution in the FLL state.

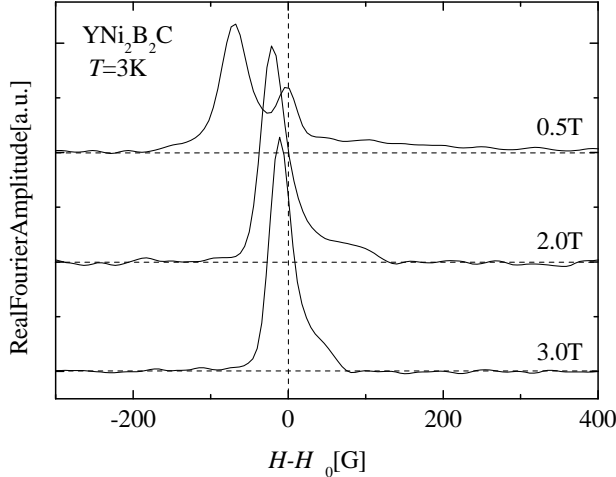


FIG. 1. Fourier Transform of the μ SR time spectra in $\text{YNi}_2\text{B}_2\text{C}$ at 3 K with a strong apodization (see text).

Figure 1 shows the fast Fourier transforms (FFT) of the muon precession signal in $\text{YNi}_2\text{B}_2\text{C}$ for different fields at $T \simeq 3.0$ K with strong apodization¹⁰. The real amplitude of the FFT corresponds to the internal magnetic field distribution in the FLL state convoluted with an additional damping to account for the weak nuclear dipolar fields, FLL disorder, and distortions originating from the finite time window and the reduced statistics at later times.¹¹ The high-field cutoff reflecting the magnetic field at the vortex core is clearly observed. The small peak near $H - H_0 = 0$ is the residual background generated by muons which missed the sample.

In our preliminary analysis¹², it was revealed that the local London model with a square FLL fails to reproduce the observed μ SR spectra in $\text{YNi}_2\text{B}_2\text{C}$. More specifically, the apex angle θ of the FLL gradually increases from 60° with increasing field, but it levels off over the field range above 0.5 T with $\theta \simeq 75^\circ$ (see Fig. 4(c)) where the square FLL is established by other measurements (i.e., $\theta \simeq 90^\circ$)^{7,13-15}. Thus, the result in Ref. 12 was obtained with $\theta \simeq 75^\circ$ for $H > 0.5$ T. As it is demonstrated below, we have found that this problem is alleviated by taking account of the nonlocal corrections⁹. The local magnetic field at any point in the \hat{a} - \hat{b} plane is

$$H(\mathbf{r}) = \overline{H}_0 \sum_{\mathbf{K}} \frac{e^{-i\mathbf{K}\cdot\mathbf{r}} e^{-K^2\xi_v^2}}{1 + K^2\lambda^2 + \lambda^4(0.0705CK^4 + 0.675Ck_x^2k_y^2)}, \quad (1)$$

where \mathbf{K} is the reciprocal lattice vector,

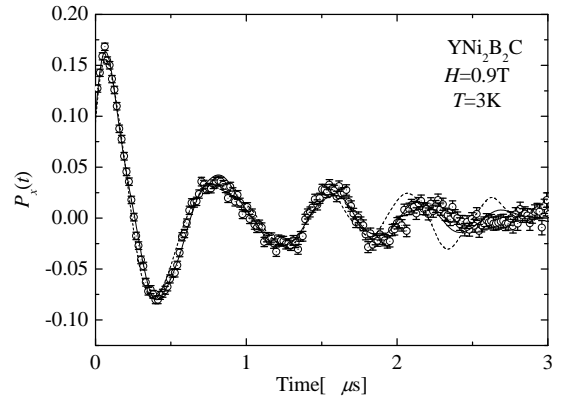


FIG. 2. The muon precession signal $P_x(t)$ in $\text{YNi}_2\text{B}_2\text{C}$ at $H = 0.9$ T, displayed in a rotating-reference-frame frequency of ~ 2 MHz. For the solid/dashed curves, see the text.

$$\mathbf{K} = l\mathbf{k}_x + m\mathbf{k}_y, \quad (l, m = 0, \pm 1, \pm 2, \dots) \quad (2)$$

$$\mathbf{k}_x = \frac{2\pi}{a \sin \theta} \begin{pmatrix} -\cos \frac{\theta}{2} \hat{x} + \sin \frac{\theta}{2} \hat{y} \end{pmatrix} \quad (3)$$

$$\mathbf{k}_y = \frac{2\pi}{a \sin \theta} \begin{pmatrix} \cos \frac{\theta}{2} \hat{x} + \sin \frac{\theta}{2} \hat{y} \end{pmatrix}, \quad (4)$$

with \hat{x} and \hat{y} being the plane of precession, a the FLL parameter, θ the apex angle of the FLL, \overline{H}_0 the average magnetic field, λ the magnetic penetration depth, and ξ_v being the cutoff parameter. The above reciprocal lattice vectors correspond to the case where the diagonal direction of the FLL ($= \mathbf{u} + \mathbf{v} = 2\sin \frac{\theta}{2} \hat{x}$) is along the $\langle 100 \rangle$ direction of the crystal axis. The anisotropic parameter C is determined by the band structure, in which C scales with λ as $C = C_0/\lambda^2$.⁹ The coefficients for C in Eq.(1) were adopted from the theoretical estimation for $\text{LuNi}_2\text{B}_2\text{C}$.⁹ The local London model is obtained by putting $C = 0$.

In addition to the nonlocal corrections, we have developed a program to analyze the μ SR spectra in the *time* domain to eliminate the uncertainty in the estimation of statistical errors associated with fitting the FFT spectra. The theoretical time evolution of the muon spin polarization was generated by assuming the field profile of Eq. (1)¹¹,

$$P_x(t) + iP_y(t) = \int \frac{d\mathbf{r}}{dH(\mathbf{r})} \exp(i\gamma_\mu H(\mathbf{r})t) dH \quad (5)$$

(γ_μ is the muon gyromagnetic ratio) and compared with the time spectra by the chi-square (χ^2) minimization technique. Considering the results of small angle neutron scattering (SANS)^{7,13,14} and scanning tunneling microscopy/spectroscopy (STM/STS)¹⁵, the apex angle θ was fixed to 90° for $H \geq 0.4$ T while it was treated as a fitting parameter for $H < 0.4$ T.

A typical example of the μ SR time spectra measured in $\text{YNi}_2\text{B}_2\text{C}$ under a magnetic field of 0.9 T is shown in Fig. 2, where the solid curve is a fit by the nonlocal London model while the dashed curve is by the local model with

the apex angle fixed to 90° . The value of deduced χ^2 for the nonlocal model is more than three times smaller than that for the local model, indicating that the nonlocal model provides much better description of the data. The rate of additional Gaussian relaxation due to trivial sources (nuclear dipolar fields, vortex pinning, etc.) is about $0.34 \mu\text{s}^{-1}$ at 0.9 T and it tends to be independent of the field. Figure 3 shows the contour plot of $H(\mathbf{r})$ around a vortex at $H = 0.9$ T reproduced from μSR data, where the $\langle 100 \rangle$ axis of the crystal is along the horizontal direction. The fourfold symmetry due to the nonlocal corrections in Eq.(1) is clearly observed. We note that there are two possible orientations of the FLL configuration in Eq.(1), where the diagonal direction $\mathbf{u} + \mathbf{v}$ is parallel with either the $\langle 100 \rangle$ or the $\langle 110 \rangle$ crystalline axis. We have found that the field distribution with $\mathbf{u} + \mathbf{v}$ parallel with $\langle 110 \rangle$ does not reproduce our data with any combination of parameters. This is perfectly in line with the results of other experiments, as well as the theoretical calculation which yields a lower free energy for $\mathbf{u} + \mathbf{v}$ parallel with $\langle 100 \rangle$.⁹

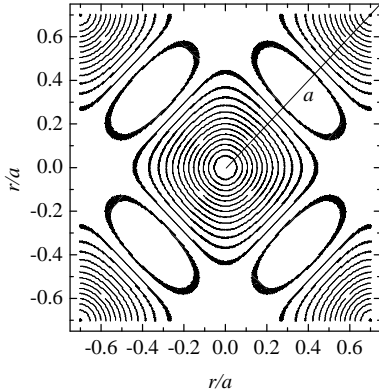


FIG. 3. The contour map of a flux-line at $H = 0.9$ T in real space, where the unit cell length a of FLL is 471.9 \AA .

The physical parameters λ , ξ_v , θ and C versus normalized external field at 3 K are shown in Fig. 4. We treated C as a fitting parameter because its value in $\text{YNi}_2\text{B}_2\text{C}$ is unknown. The λ in $\text{YNi}_2\text{B}_2\text{C}$ clearly exhibits a *linear* H -dependence. A fit to the relation $\lambda(h) = \lambda(0)(1 + \eta \cdot h)$, ($h = H/H_{c2}$) provides a dimensionless parameter η that represents the strength of the pair-breaking effect. We obtain $\eta = 0.97$ (with $\lambda(0) = 567.8 \text{ \AA}$) which is slightly smaller than that in NbSe_2 (i.e., $\eta = 1.61$ at $0.33T_c^3$). The cutoff parameter ξ_v (Fig. 4(b), solid squares) shows a steep decrease with increasing H and subsequently levels off at $h \equiv H/H_{c2} > 0.1$ ($H > 0.7$ T). In our preliminary analysis¹², we interpreted this cutoff parameter as ρ_v (see eq. (2) in Ref. 12). In the field region $h < 0.06$ where θ was set as a free parameter, θ gradually decreases with decreasing field, indicating that the FLL transforms into a nearly hexagonal lattice. However, θ does not reach 60° in the lowest magnetic field. The anisotropy C decreases with increasing H , where it

exhibits little correlation with θ . While the value at lower field is close to the theoretical estimation (~ 0.22 at 0.05 T in $\text{LuNi}_2\text{B}_2\text{C}$ ⁹), we found that $C\lambda^2$ tends to decrease with increasing field.

The field profile in Fig. 3 implies that there is an anisotropy between the $\langle 100 \rangle$ and $\langle 110 \rangle$ directions in the effective length scales (λ and ρ_v), whereas the model parameters in Eq.(1) represent mean values. Moreover, special precaution must be taken to interpret the parameters in Eq.(1) upon the introduction of nonlocal corrections involving the higher order terms of K , where the definition of these length scales are modified from those found in the previous analysis with local London models, making it unsuitable to compare directly. In order to evaluate ρ_v including the effect of anisotropy, we calculated the supercurrent density $J(r)$ from the deduced $H(r)$ using Maxwell's relation $J(\mathbf{r}) = |\nabla \times \mathbf{H}(\mathbf{r})|$. The radius ρ_v was then defined as the distance from the vortex center for which $J(r)$ reaches its maximum value. The estimated values are $\rho_{v\langle 100 \rangle} = 66.7 \text{ \AA}$ and $\rho_{v\langle 110 \rangle} = 70.8 \text{ \AA}$, yielding the ratio $\rho_{v\langle 100 \rangle} / \rho_{v\langle 110 \rangle} = 0.942$.

The field dependence of ρ_v is shown in Fig. 4(b). The values of ρ_v are systematically larger than ξ_v , suggesting that it may not be appropriate to interpret the cutoff parameter as the vortex core radius, whereas we assumed that $\rho_v = \xi_v$ in the previous analysis¹². We stress that the core radius can be obtained directly from the field profile $H(\mathbf{r})$ deduced from the μSR data, independent of the details of the FLL model used.¹¹ Having said this, the field dependence of ρ_v is qualitatively similar to that of ξ_v , showing a steep decrease with increasing field in the field range $H/H_{c2} < 0.15$.

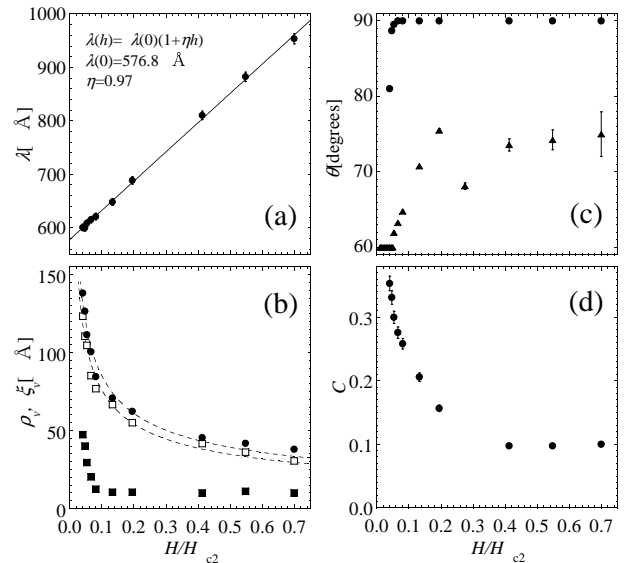


FIG. 4. The H dependence of (a) λ , (b) ρ_v determined by μSR where $\rho_{v\langle 100 \rangle}$ is shown by open squares, $\rho_{v\langle 110 \rangle}$ by solid circles and ξ_v by solid squares, (c) θ by circles and the one deduced from the local London model¹² by triangles, and (d) C in the FLL state of $\text{YNi}_2\text{B}_2\text{C}$ at 3 K. The dashed curves in (b) are described in the text.

Recent calculations for s -wave superconductors based on the quasiclassical Eilenberger equations predicts a shrinkage of ρ_v due to vortex-vortex interactions.¹⁶ The quasiparticle density of states (DOS) $N(H)$ is proportional to H^β with $\beta = 0.67$ at $T = 0$ in their prediction. Provided that all the DOS comes from inside the vortex cores, we would expect

$$N(H) = N_{\text{core}}(H) \propto \pi \rho_v^2 \cdot H \propto H^\beta \quad (6)$$

where the factor H arises from the number of vortices per unit area, and $\rho_v \propto H^{(\beta-1)/2}$. Fitting the field dependence of $\rho_{v\langle 100 \rangle}$ and $\rho_{v\langle 110 \rangle}$ in Fig. 4(b) to the relation $\rho_v = \rho_0 h^{(\beta-1)/2}$ yields $\beta_{\langle 100 \rangle} = 0.026$, $\rho_{0\langle 100 \rangle} = 24.7 \text{ \AA}$ and $\beta_{\langle 110 \rangle} = 0.014$, $\rho_{0\langle 110 \rangle} = 27.1 \text{ \AA}$, while the field dependence of $\gamma(H)$ yields $\beta = 0.430 \equiv \beta_{\text{SH}}^2$. The considerably smaller values for $\beta_{\langle 100 \rangle}$ and $\beta_{\langle 110 \rangle}$ compared with β_{SH} or the theoretical prediction strongly suggests that the origin of the \sqrt{H} behavior of $\gamma(H)$ is related to the quasiparticle excitations outside the vortex cores. This is in marked contrast with the case of CeRu_2 where $\beta \simeq \beta_{\text{SH}}$, indicating that the DOS is mostly attributed to the quasiparticles within the vortex cores.⁴ The existence of delocalized quasiparticle excitations is further suggested by the fact that de Haas-van Alphen effect has been clearly observed in the mixed state of $\text{YNi}_2\text{B}_2\text{C}$, where the cyclotron radius is much larger than the coherence length ξ .¹⁷ Surface impedance Z_s measurements also indicate delocalized quasiparticles outside the vortex cores.¹⁸ The magnetic field dependence of $N(H)$ inside the cores estimated by Z_s is proportional to H , except at very low field. These results are consistent with our conclusion that the localized quasiparticles within the vortex cores (determined by ρ_v) contribute little to the \sqrt{H} behavior of the Sommerfeld constant, at least for $h > 0.15$. Here, we note that the agreement between β and β_{SH} is improved by assuming that $N(H) \propto \rho_v \cdot H$ instead of Eq. (6)¹⁹, although the microscopic origin of this linear relation is not obvious at this stage. In any case, the small β and associated steeper field dependence of ρ_v at lower fields might be partly explained by the multi-band effect, where the electronic structure is effectively described by a two-band model²⁰. The BCS coherence length $\xi_0 = \hbar v_F / \pi \Delta_0$ (where $\rho_v \leq 0.6 \xi_0$ ¹⁶) estimated from the Fermi velocity v_F and the energy gap Δ_0 in $\text{YNi}_2\text{B}_2\text{C}$, is 60 to 120 \AA for one group and 370 \AA for another branch, suggesting that $\rho_v(H \rightarrow 0)$ is controlled by the larger value of ξ_0 . We also note a possible connection to the anisotropic energy gap in $\text{YNi}_2\text{B}_2\text{C}$ reported by photoemission spectroscopy²¹, where ξ_0 is scaled by the magnitude of Δ_0 .

Finally, we discuss the apex angle θ at lower fields where the deviation from a hexagonal lattice is expected ($h < 0.04$). We found that the agreement between the measured field distribution and calculations based on the present model becomes far from satisfactory in the field range at $h < 0.04$ ($H < 0.3$ T). This is probably due to the presence of the deep minima along the $\langle 110 \rangle$ direction

in Fig. 3, which persists irrespective of the apex angle (Note that the square shaped field distribution is independent of θ , as is evident in Eq.(1)). The poor agreement strongly suggests that Eq.(1) gives the true ground state only for the case of a square FLL, while the more isotropic distribution would be realized at lower fields as the $\theta \simeq 60^\circ$ well reproduced by the local London model¹². Thus, a more refined model is needed to reproduce the complete evolution of the FLL with field. We also point out the possibility that FLL domains present through the hexagonal-to-square transition (like in $\text{LuNi}_2\text{B}_2\text{C}$ ²²) play an important role.

In summary, we found that ρ_v shrinks steeply with increasing field while λ depends linearly on the magnetic field, strongly suggesting the presence of excess quasiparticles outside the vortex cores at higher fields. These results indicate the need to reconsider the conventional picture of a rigid normal-electron core by taking into account the vortex-vortex interactions mediated by delocalized quasiparticles.

We thank the TRIUMF μSR staff for technical support. This work was partially supported by a JSPS Research Fellowships for Young Scientists, Japan, by a Grant-in-Aid for Science Research on Priority Areas from the Ministry of Education, Culture, Sports, Science, and Technology, Japan and also by a Grant from the CREST, JST, Japan.

[†] Also at School of Mathematical and Physical Science, The Graduate University for Advanced Studies

¹ M. Hedo, *et al.*, J. Phys. Soc. Jpn. **67**, 272 (1998).

² M. Nohara, *et al.*, J. Phys. Soc. Jpn. **68**, 1078 (1999).

³ J.E. Sonier, *et al.*, Phys. Rev. Lett. **79**, 1742 (1997).

⁴ R. Kadono, *et al.*, Phys. Rev. B **63**, 224520 (2001).

⁵ U. Yaron, *et al.*, Nature **382**, 236 (1996).

⁶ M.R. Eskildsen, *et al.*, Phys. Rev. Lett. **78**, 1968 (1997).

⁷ D.McK. Paul, *et al.*, Phys. Rev. Lett. **80**, 1517 (1998).

⁸ M.R. Eskildsen, *et al.*, Nature **393**, 242 (1998).

⁹ V.G. Kogan, *et al.*, Phys. Rev. B **55**, R8693 (1997).

¹⁰ R.H. Norton *et al.*, J. Opt. Sci. Soc. Am. **66**, 259 (1976); **67**, 419 (1976).

¹¹ J.E. Sonier, *et al.*, Rev. Mod. Phys. **72**, 769 (2000).

¹² K. Ohishi, *et al.*, Physica B **289-290**, 377 (2000).

¹³ M. Yethiraj, *et al.*, Phys. Rev. Lett. **78**, 4849 (1997).

¹⁴ M. Yethiraj, *et al.*, Phys. Rev. B **58**, R14767 (1998).

¹⁵ H. Sakata, *et al.*, Phys. Rev. Lett. **84**, 1583 (2000).

¹⁶ M. Ichioka, *et al.*, Phys. Rev. B **59**, 184 (1999).

¹⁷ T. Terashima, *et al.*, Phys. Rev. B **56**, 5120 (1997).

¹⁸ K. Izawa, *et al.*, Phys. Rev. Lett. **86**, 1327 (2001).

¹⁹ J. E. Sonier, *et al.*, Phys. Rev. Lett. **82**, 4914 (1999).

²⁰ S. V. Shulga, *et al.*, Phys. Rev. Lett. **80**, 1730 (1998).

²¹ T. Yokoya, *et al.*, Phys. Rev. Lett. **85**, 4952 (2000).

²² L.Ya. Vinnikov, *et al.*, Physica B **284-288**, 813 (2000)